Ultrasonics 98 (2019) 62–71

Contents lists available at ScienceDirect

Ultrasonics

journal homepage: www.elsevier.com/locate/ultras

Sonothrombolysis with magnetic microbubbles under a rotational magnetic field

Bohua Zhang[a], Howuk Kim[a], Huaiyu Wu[a], Yu Gao[b], Xiaoning Jiang[a,*]

[a] Department of Mechanical and Aerospace Engineering, North Carolina State University, Raleigh 27695, NC, USA
[b] Institute of Advanced Materials, Nanjing University of Posts and Telecommunications, Nanjing 210023, China

ARTICLE INFO

Keywords:
Magnetic microbubbles
Magnetic nanoparticle
Thrombolysis
Sonothrombolysis
Cavitation

ABSTRACT

Thrombosis is an extremely critical clinical condition where a clot forms inside a blood vessel which blocks the blood flow through the cardiovascular system. Previous sonothrombolysis methods using ultrasound and microbubbles (MBs) often have a relatively low lysis rate due to the low microbubbles concentration at clot region caused by blood flow in the vessel. To solve this problem, the magnetic microbubbles (MMBs) that can be retained by an outer magnetic field against blood flow are used in this study. Here we report the development of a new method using the rotational magnetic field to trap and vibrate magnetic microbubbles at target clot region and then using an intravascular forward-looking ultrasound transducer to activate them acoustically. In this study, we investigated the influence of different blood flow conditions, vessel occlusion conditions (partial and fully occluded), clot ages (fresh, retracted), ultrasound parameters (input voltage, duty cycle) and rotational magnetic field parameters (amplitude, frequency) on the thrombolysis rate. The results showed that the additional use of magnetic microbubbles significantly enhances *in vitro* lysis of blood clot.

1. Introduction

Stroke is a significant cause of mortality, accounting for 11.8% of total deaths worldwide [1]. Most of the strokes are caused by an occlusion to a blood vessel in the brain which can damage surrounding tissue [2]. Thrombolysis is a process of breaking up and dissolving blood clots which can help salvage affected tissue and improves the clinical outcome [3]. At present, the FDA approved thrombolytic agent is recombinant tissue-type plasminogen (rt-PA) [4]. However, rt-PA based treatment may trigger fatal side effects such as the increased risk of intracranial hemorrhage (ICH) [5]. As a result, intravenous rt-PA administration is subject to rigid criteria, and the rt-PA drug is only suggested within the first 3 h following onset of stroke, which is a very limited therapeutic time frame for patients [6]. Patients who are ineligible for rt-PA are usually treated with thrombectomy, which is currently only used at comprehensive stroke centers and limited to a large diameter artery [7].

Recently, sonothrombolysis (STL), a technique involving the use of microbubbles (MBs) combined with ultrasound (US) to enhance clot dissolution, is under therapeutic assessment as a method for recanalization of occluded blood vessels. Over the past twenty years, many case-control studies and clinical trials have demonstrated that sonothrombolysis with microbubbles is a relatively safe and effective thrombolytic treatment in ischemic stroke compared to rt-PA only based therapy [8,9]. Ultrasound thrombolysis with injected microbubble agents may allow a reduced administered rt-PA dose and minimize the side-effects on tissue and blood vessels, enabling the thrombolysis treatment to become more efficient and safer. The current study showed that acoustic waves with frequencies range from sub-MHz to 1 MHz and intensities below the threshold of inertial cavitation are critical to stable cavitation of microbubbles [10]. Furthermore, the previous study showed that a higher microbubble concentration would lead to greater clot disruption because of the higher number of microbubbles cavitating in response to US pressure [11]. Besides, to promote and sustain the nucleation of cavitation during US treatment process, a higher dose ($> 1.2 \times 10^{10}$ MBs/mL) of MBs are recommended for better thrombolytic treatment [12].

One of the significant challenges in the process of sonothrombolysis treatment is to control the hydrodynamic conditions in occluded vessels since they mostly limit the number of microbubbles that can be retained and cavitated at the site of a blood clot during ultrasound exposure. The low concentration of microbubbles due to the blood flow will potentially decrease the thrombolysis rate. Therefore, there are emerging studies focusing on the development of microbubble targeting technique which is a promising method that could increase the proximity between microbubble agents and the blood clot surface, thus increasing

* Corresponding author.
E-mail address: xjiang5@ncsu.edu (X. Jiang).

https://doi.org/10.1016/j.ultras.2019.06.004
Received 2 January 2019; Received in revised form 28 March 2019; Accepted 9 June 2019
Available online 10 June 2019
0041-624X/

the thrombolysis rate and reducing the required drug dose. There are biological methods using microbubbles with antibody conjugation on their surface for targeting thrombus treatment, but those methods still rely on the passive blood flow to accumulate the microbubbles to the thrombus surface [13–17]. The acoustic radiation force can also be used to increase the accumulation efficacy of targeted microbubbles since the microbubbles can travel in the direction of sound wave propagation and aggregate at the thrombus surface [18–20]. However, the above methods are mostly dependent on the blood flow conditions and precise alignment of the beam with a target vessel, which may be challenging with complex vessels *in vivo* treatment.

As an alternative, a significant amount of investigations in recent years have focused on the development of magnetic microbubbles (MMBs) [21–24]. Magnetic microbubbles are microbubbles coated with superparamagnetic iron oxide nanoparticles that can maintain the acoustic properties of MBs and possess the sensitivity to magnetic fields. The dual-modality functionality makes MMBs useful for a broad range of application such as targeted drug delivery [21,25] and thrombolysis [26,27]. However, there are some challenging problems of using MMBs for targeted thrombolysis such as how to build a controllable magnetic system with enough strength of magnetic field and gradient to counteract blood flow in a blood vessel. Although recent studies showed the lipid-coated microbubbles with iron oxide nanoparticles can be retained with a magnet against clinically relevant flow conditions [28], there is a lack of systematic study of ultrasound thrombolysis using MMBs under magnetic field.

The present study is the first to utilize magnetic microbubbles for ultrasound thrombolysis under a rotational magnetic field (RMF). Our approach investigates whether magnetic microbubbles can be a useful adjuvant to the current microbubble-mediated sonothrombolysis treatment. We hypothesize that by oscillating magnetic microbubbles in the rotational magnetic field, a vortex-like microstreaming in clot region will enhance microbubble cavitation under sonication. In this proof-of-concept study, we aim to demonstrate the feasibility of using the rotational magnetic field to entrap and oscillate the MMBs with intravascular forward-looking ultrasound transducers for sonothrombolysis *in vitro*. First, we compared the influence of blood flow conditions on the different thrombolysis treatment methods (MB + US, MMB + US, MMB + RMF, MMB + US + RMF). Second, we investigated the influence of different clot conditions (partial occlusion, fully occluded) and different clot ages (fresh, retracted) on the thrombolysis efficiency. Finally, to better understand the mechanism of rotational magnetic field assisted sonothrombolysis, we explored the influence of various ultrasound parameters (input voltage, duty cycle) and magnetic field parameters (amplitude, frequency) on the thrombolysis rate.

2. Material and methods

2.1. Transducer development

In this study, we employ the previous forward-looking stacked ultrasound transducer design [29], and the ultrasound frequency was chosen as 620 kHz. The details of the forward-looking transducer development procedure can be found in our previous work [29]. Briefly, a stacked piezoelectric transducer which has six layers was fabricated using PZT-5A ceramic thin plates with alternating poling directions. Each PZT-5A layer thickness was 250 μm, and the total thickness of the stacked transducer was 1.6 mm without a matching layer. To bond the layer, a conductive bond (E-solder 302) was used, and the bonding layer thickness was 30 μm. The transducer has a lateral dimension of 1.2 mm and can be mounted on an 8F catheter for the intravascular test.

2.2. Blood clot preparation

The blood clots were prepared following a similar procedure used in our previous work [29]. First, the fresh bovine blood obtained from Densco Marketing, Inc. (Wood- stock, IL, USA) was mixed with 2.75% W/V $CaCl_2$ solution (Fisher Scientific, Fair Lawn, NJ) in a volume ratio of 10:1 (50 mL blood /5 mL $CaCl_2$ solution). Second, the mixed blood solution was drained to Tygon tubes (6.35 mm ID, 7.94 mm OD). Then the Tygon tubes were immersed in a 37 °C water bath for 3 h. Finally, the tubes with coagulated blood were stored at low temperature (4 °C) for 1 to 7 days to generate clots with different ages. Clot samples for thrombolysis tests were cut into a cylindrical shape (length: 12 ± 2 mm, diameter 3 ± 0.5 mm) and weighted as 130 mg ± 10% in mass and then positioned into a customized polydimethylsiloxane (PDMS) blood vessel mimicking phantom (microchannel, ID: 2–3 mm with 33.3% stenosis) as shown in Fig. 2.

2.3. Magnetic microbubble preparation

The magnetic microbubbles were prepared by a similar procedure as described in reference [24]. First, Magnetic nanoparticles (Fe_3O_4, with diameter around 50 nm, Sigma- Aldrich, St Louis, MO, USA) were mixed with deionized water to form a 2 mg/mL stock solution and then treated with ultrasound for 20 min. Second, a solution containing 400 μl of a stock solution of Fe_3O_4 nanoparticles, 150 μl of 10 mM sodium dodecyl sulfate (SDS) and 150 μl of deionized water was mixed by shaking for 1 min [24]. Finally, MMBs were left 24 h before being washed with phosphate-buffered saline (PBS) three times before use. The MMBs had an average diameter of ~6 μm.

2.4. The rotational magnetic field generation

The rotational magnetic field was generated by rotating a NdFeB N50 permanent magnet bar (Size: 12 mm * 6 mm * 3 mm) which was mounted on a 3D printed fixture with a 12 V DC motor (Fig. 2). By changing the rotational speed of the magnet bar, the various frequencies (0–25 Hz) alternating magnetic fields were generated. Compared with electromagnet made of coils, the permanent magnet has many advantages such as high magnetic flux density, no need for large power supply and coils cooling. As shown in Fig. 2, the DC motor was positioned below the PDMS phantom, and the magnetic field was aligned along the vertical direction. The magnetic field was measured by a gaussmeter (Model GM2, AlphaLab, Inc.) and the position of the DC motor was controlled by a 3-axis motion stage so that the amplitude of magnetic field applied to the clot can be adjusted by changing the distance between magnet bar and clot area.

To better understand the physics of the rotational magnet field, the magnetic field generated by the permanent magnet was simulated in the COMSOL® Multiphysics software. The simulated magnetic flux density of the magnet in the YZ plane is shown in Fig. 1 (A). The white arrow direction represents the direction of the magnetic flux density norm. Fig. 1 (B) showed the relationship between rotational magnetic flux density (B) and the distance (d) from the rotating magnet. The measured results agree well with the simulation ones. Fig. 1 (C) showed the magnetic flux density change when the magnet rotated from 0 degrees to 180 degrees. When the magnet was rotated by a DC motor, the rotational magnetic field could be generated in a pattern as shown in Fig. 1 (C). The magnetic field generated a torque $\vec{\tau} = \vec{\mu} \times \vec{B}$. This induced the rotation of the magnetic microbubbles around their own axis and the rotation speed can be controlled by changing the rotational magnetic field frequency.

2.5. In vitro tests procedure

As shown in Fig. 2, for every treatment test, a 130 mg ± 10% clot sample was positioned into a 3 mm diameter PDMS microchannel. The PDMS microchannel was filled with saline at a temperature of 37.3 ± 0.3 degreesC. The saline was pumped by a peristaltic liquid

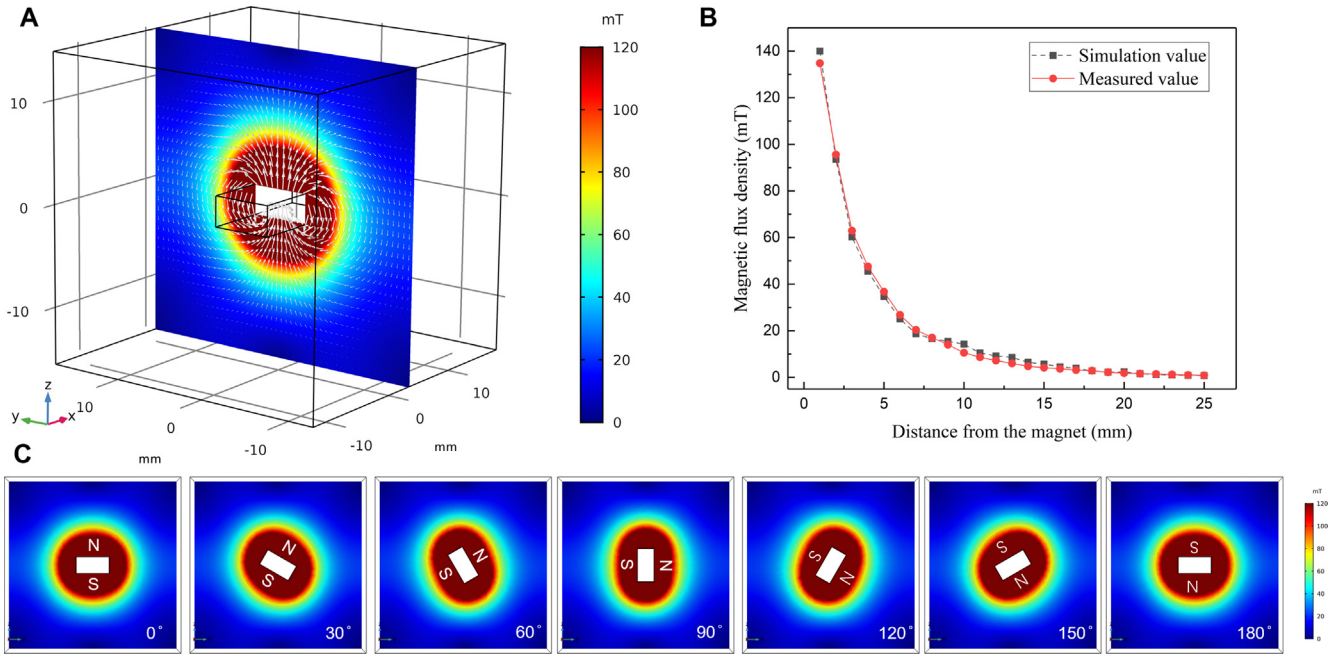

Fig. 1. Simulation of the magnetic field created by permanent magnet bar in the YZ plane. (A) The magnetic flux density of the permanent magnet (white arrow represents the direction of the magnetic flux), (B) The rotational magnetic flux density of the magnet used for generating a rotational magnetic field at different distances, (C) The magnetic flux density changes when the magnet rotates 180 degrees.

pump (INTL-LAB, China) from a saline reservoir into the flow inlet of the PDMS microchannel. The liquid pressure inside the microchannel tube was measured by a low-pressure gauge (200 series, Noshok, Inc) and kept at 3.7 mmHg pressure level by controlling the speed of the pump. The flow outlet of the microchannel tube was connected to a reservoir to collect the liquid and debris after the thrombolysis treatment. A thermocouple probe (OMEGA Engineering, Norwalk, CT) was placed on the PDMS microchannel and the probe tip was positioned at the clot region to measure the temperature change during the treatment. The ultrasound transducer was inserted through the right side of the PDMS microchannel tube, and the transducer position was controlled by a 3-axis motion stage to control the distance between the transducer and the clot (~0.5 mm). The NdFeB magnet mounted on a DC motor was controlled by a motor speed controller and was positioned under the PDMS microchannel to apply the alternating magnetic field to the magnetic microbubbles. The US transducer was driven by a 53 dB RF power amplifier (75A250A, AR, Inc. Souderton, PA) and the input signal was generated by a function generator (33250A, Agilent Technologies, Inc., Loveland, CO). To pump the magnetic microbubbles into the tube, a micropump (DUAL-NE-1010-US, New Era Pump Systems Inc., Farmingdale, NY) was used, and the flow rate was maintained at 100 µl/min. Diluted magnetic microbubbles (10^9/mL) with average diameters of ~6 µm were used as the therapeutic agents with the treatment time of 30 min for each test.

To investigate the influence of flow pressure conditions on different thrombolysis treatment, the fully occluded blood clot flow model was used in this test. First, the blood clot was cut into the small size cylindrical shape (length: 12 ± 2 mm, diameter 3 ± 0.5 mm) and

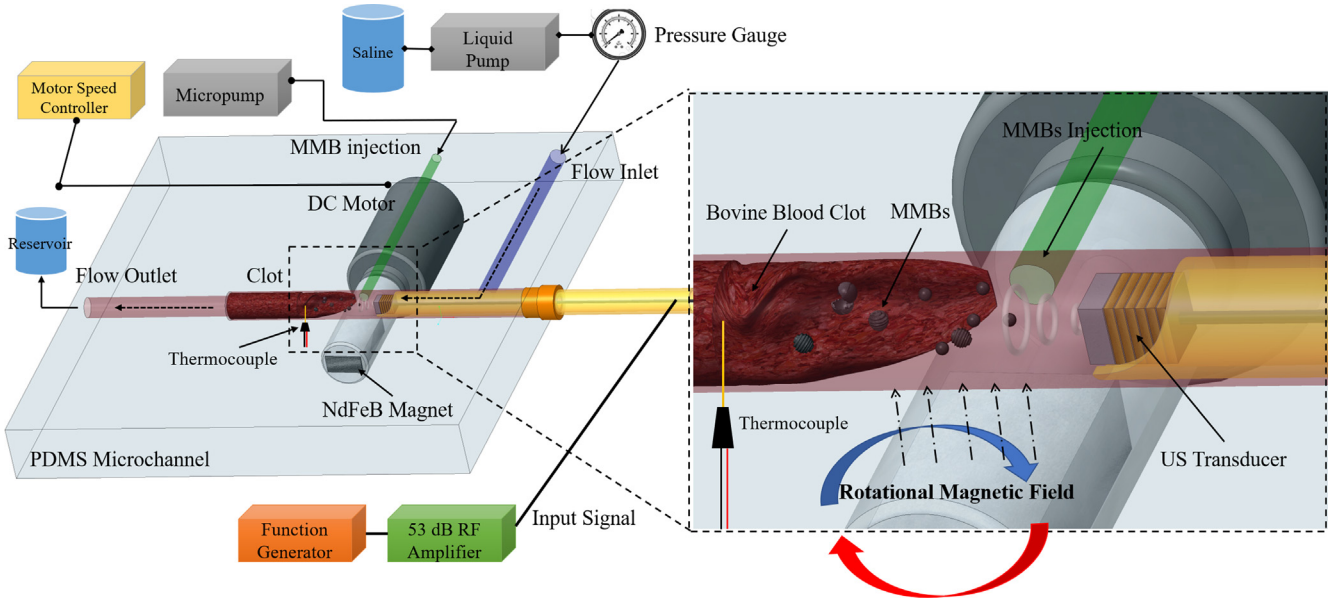

Fig. 2. *In vitro* ultrasound thrombolysis with magnetic microbubble under a rotational magnetic field experiment setup.

weighted as 130 mg ± 10% in mass and then positioned into a PDMS microchannel as shown in Fig. 2. Then the saline flow was pumped into the microchannel tube. Since the microchannel was fully occluded by the blood clot before the treatment, there will be no flow out from the outlet of the microchannel. The liquid pressure in the fully occluded microchannel was measured and maintained at 3.7 mmHg. Second, the magnetic microbubbles (concentration: 10^9/mL, average diameter ~6 μm) were injected through a 1 mm PDMS microchannel tube by a micropump. Then the rotational magnetic field (RMF) with magnetic flux density B = 50 mT and frequency f = 20 Hz generated by rotating a NdFeB magnet was applied to the clot area to activate the magnetic microbubble. Third, the US transducer with input signal as 120 V_{pp} input voltage and 10% duty cycle was position near the clot surface (~0.5 mm) to cavitate the magnetic microbubble for the thrombolysis treatment. To compare the influence of ultrasound and rotational magnetic field on the thrombolysis treatment process, different groups of treatment methods were conducted under the same procedure described above. To be specific, the control group was only injected with magnetic microbubble with-out any ultrasound and magnetic field exposure. The MB + US group was treated with microbubble (MB concentration: 10^9/mL, average diameter ~6 μm) and ultrasound. The MB was prepared by a similar process in our previous work [29]. The MMB + US group was treated with magnetic microbubble and ultrasound only. The MMB + RMF group was treated with magnetic microbubble (MMB) and rotational magnetic field (RMF) only. The MMB + US + RMF was treated with magnetic microbubble and both ultrasound and rotational magnetic field. The similar treatments were also repeated without the flow pressure in fully occluded microchannel to compare the results with the presence of flow pressure.

Moreover, to clarify the influence of flow model on the thrombolysis treatment, different clot occlusion conditions were investigated. As shown in Fig. 3, the clot was cut into different size to meet the requirement for different occlusion case (40% partial occlusion, 70% partial occlusion, 100% fully occluded). The similar flow pressure conditions and treatment methods as described above were used in this experiment. To investigate the influence of clot ages on the thrombolysis treatment, different clots with ages from 1 day to 7 days were used in the experiment with similar flow pressure conditions and treatment methods.

Finally, to clarify the thrombolysis effect of ultrasound, rotational magnetic field and magnetic microbubble combined treatment, various treatment cases were considered. The blood clots were exposed to ultrasound with different duty cycle (1.6%, 3.2%, 6.4%, 10%), input voltage (26 V_{pp}, 39 V_{pp}, 45 V_{pp}, 62 V_{pp}, 68 V_{pp}, 80 V_{pp}, 93 V_{pp}, 120 V_{pp}) and rotational magnetic fields with various magnetic flux density (4 mT, 10 mT, 30 mT, 50 mT, 65 mT, 80 mT), and frequency (static, 1 Hz, 5 Hz, 10 Hz, 15 Hz, 20 Hz, 25 Hz). The results presented in this study were expressed as the mean ± SD (n = 3). Statistical analysis was conducted using the MATLAB Statistical Toolbox (Mathworks, Natick, MA, USA). The student's *t*-test was used to estimate the statistical significance of tests with various treatment conditions.

3. Results and discussion

3.1. Thrombolysis with different treatment methods under flow pressure

Previously, researchers have shown that the microbubble-mediated ultrasound thrombolysis rate is also affected by blood flow pressure [29]. The flow pressure (3.7 mmHg) in this study is in the range of physiologic flow pressure in the human vein. To investigate the influence of flow pressure conditions on different thrombolysis treatment, the fully occluded blood clot flow model was used in this test. Different groups of methods (MB + US, MMB + US, MMB + RMF, MMB + US + RMF) were used for the thrombolysis treatment with the flow pressure and without the flow pressure. For each treatment, we use the same treatment parameters as 30 min treatment time, ultrasound input parameters (120 V_{pp} input voltage, 10% duty cycle, f = 620 kHz) and magnetic field parameters (magnetic field flux density B = 50 mT, magnetic field frequency f = 20 Hz). As shown in Fig. 4, among all the treatment groups, the clot mass reduction rate is slightly higher with the flow pressure than without flow pressure. This is likely because in the fully occluded flow model, the flow pressure will help the MB/MMB better penetration the clot fibrin network and achieve higher lysis rate.

Moreover, the clot mass reduction rate using magnetic microbubbles treated by the combined method of ultrasound and the rotational magnetic field is much higher than the group that treated with ultrasound only or rotational magnetic field only. The statistics result also shows there is a significant difference ($p < 0.01$) between

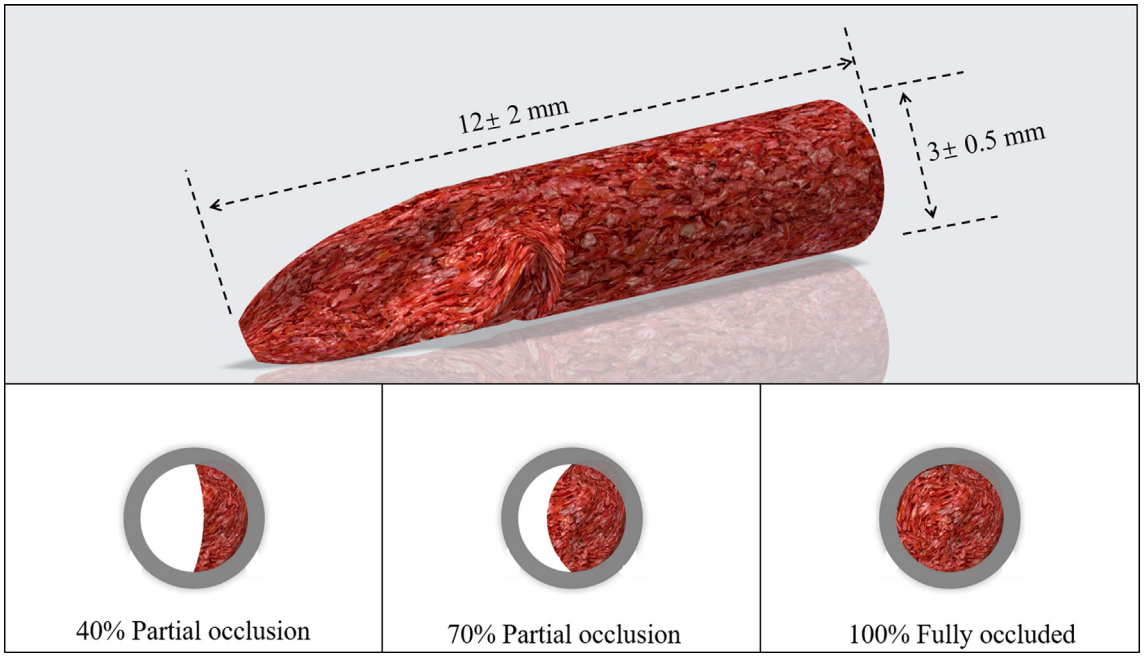

Fig. 3. Schematic of different clot occlusion (40% partial occlusion, 70% partial occlusion, 100% fully occluded).

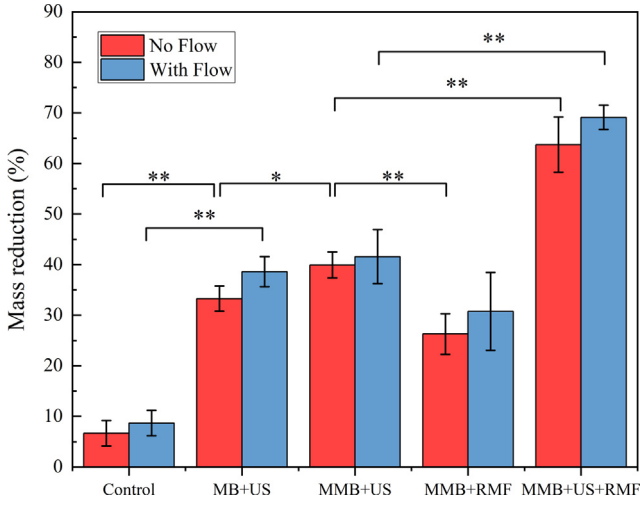

Fig. 4. *In vitro* test results using different treatment methods with or without flow pressure. (Treatment time: 30 min, ultrasound parameters: 120 V_{pp} input voltage, 10% duty cycle, f = 620 kHz, magnetic field: B = 50 mT, f = 20 Hz) (*P < 0.05, **P < 0.01).

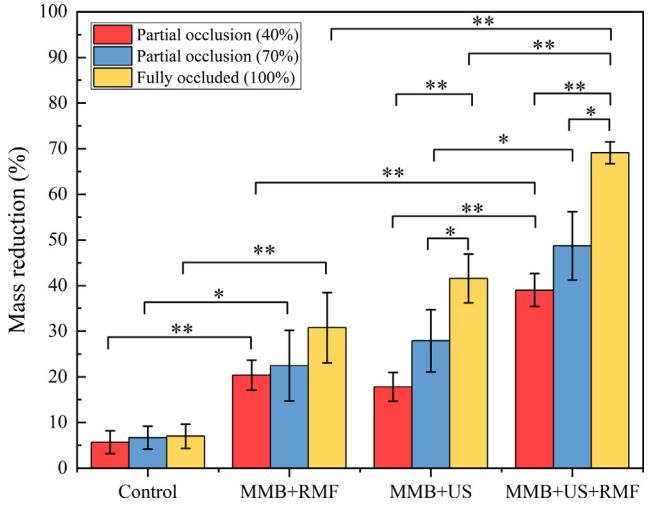

Fig. 6. *In vitro* test results using different treatment methods with different vessel occlusion case. (Treatment time: 30 min, ultrasound parameters: 120 V_{pp} input voltage, 10% duty cycle, f = 620 kHz, magnetic field: B = 50 mT, f = 20 Hz) (*P < 0.05, **P < 0.01).

MMB + US group and MMB + US + RMF group. This indicates that the rotational magnetic fields applied on the magnetic microbubble could enhance the ultrasound thrombolysis treatment.

The *in vitro* clot lysis results using MMB + US + RMF treatment method in a fully occluded blood clot flow model with flow pressure were shown in Fig. 5. The captured images with 10 min-interval show gradual volume reduction of the blood clot. After 40 min treatment time, the target clot size reduced to about 22.2% of its original size (mass reduction from 130 mg to 30 mg) which shows that the MMB + US + RMF combined method can improve the clot lysis rate significantly.

3.2. Thrombolysis treatment with different clot occlusion case

To clarify the influence of flow model on the thrombolysis treatment, different vessel occlusion conditions were investigated. For each treatment, we use the same treatment parameters as 30 min treatment time, ultrasound input parameters (120 V_{pp} input voltage, 10% duty cycle, f = 620 kHz) and magnetic field parameters (magnetic field flux density B = 50 mT, magnetic field frequency f = 20 Hz). The control group was only injected with magnetic microbubble without any ultrasound and magnetic field exposure. As shown in Fig. 6, among all the treatment groups, the partial occlusion 40% case has the lowest clot mass reduction compared to the partial occlusion 70% case and fully occluded case. This is likely because the MMBs concentration in the partial occlusion flow model will drop due to the presence of flow. Therefore, the available magnetic microbubbles that retained in the clot surface area for the ultrasound treatment were limited to a low concentration due to the flow which resulted in a low thrombolysis rate. However, the group with combined treatment (MMB + US + RMF) still shows a higher mass reduction rate than the ultrasound only (MMB + US) group. Besides, the statistics result also shows that even in partial occlusion 40% case, there is still a significant difference ($p < 0.01$) in mass reduction rate when using combined treatment (MMB + US + RMF) (39%), compared to ultrasound only (MMB + US) (17.8%).

3.3. Thrombolysis treatment with different clot ages

According to our previous study [29], the fresh clot is considered as clot formed within 1 day and the retracted clot is considered as clot formed more than 3 days. Therefore, clot with ages from 1 day to 7 days was selected in this study to better understand the clot aging effect on the thrombolysis rate influence. To investigate the influence of clot ages on the thrombolysis treatment, the fully occluded blood clot flow model with flow pressure and the clot with different ages from 1 day to 7 days were used in this test. For each treatment, we use the same treatment parameters as 30 min treatment time, ultrasound input parameters (120 V_{pp} input voltage, 10% duty cycle, f = 620 kHz) and magnetic field parameters (magnetic field flux density B = 50 mT, magnetic field

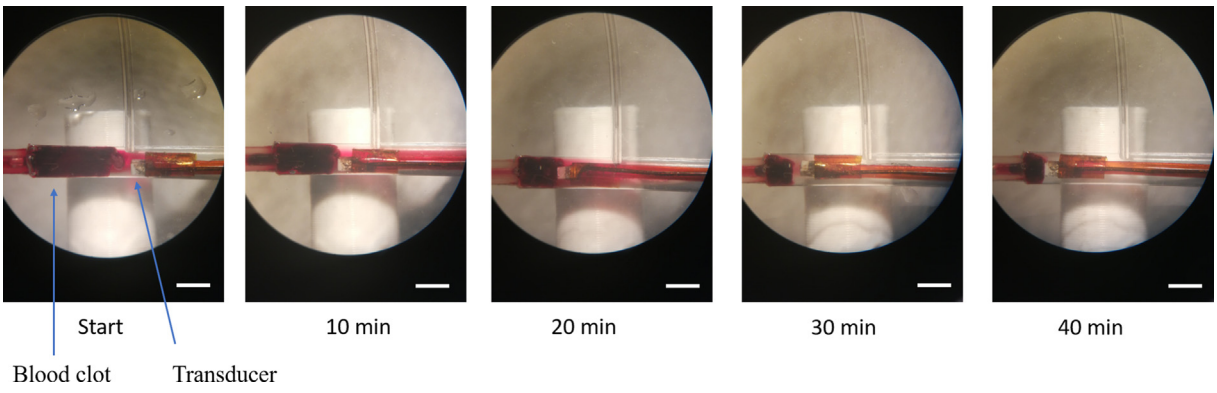

Fig. 5. *In vitro* clot lysis results. Captured images under microscope during 40 min treatment by using MMB + US + RMF treatment methods (ultrasound parameters: 120 V_{pp} input voltage, 10%duty cycle, f = 620 kHz, magnetic field: B = 50 mT, f = 20 Hz) (scale bar = 3 mm).

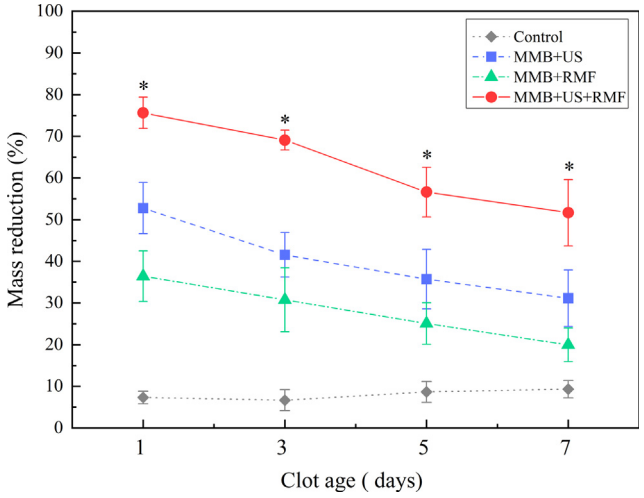

Fig. 7. *In vitro* test results using different treatment methods with different clot ages. (Treatment time: 30 min, ultrasound parameters: 120 V_{pp} input voltage, 10% duty cycle, f = 620 kHz, magnetic field: B = 50 mT, f = 20 Hz), *: statistically different between group MMB + US and group MMB + US + RMF ($P < 0.05$).

frequency f = 20 Hz). The control group was only injected with magnetic microbubble without any ultrasound and magnetic field exposure. As shown in Fig. 7, the clot mass reduction rate slightly drops when clot ages increase. This is likely because as the clot ages increase, the clot condition changes from fresh to retracted. In the retracted clot, there will be more fibrin networks that prevent clot lysis. The fresh clots are much more easily to be dissolved during the treatment. However, the combined method (MMB + US + RMF) still shows a higher mass reduction rate than the ultrasound only (MMB + US) method significantly ($p < 0.05$).

3.4. Thrombolysis treatment with different input parameters

To clarify the thrombolysis effect of ultrasound, the rotational magnetic field, and magnetic microbubble combined treatment, various treatment cases were considered. As shown in Fig. 8 (A), different duty cycles were used as the ultrasound input parameter. The result shows that the clot mass reduction will increase when the duty cycle increase. As shown in Fig. 8 (B), when the input voltage increases from 0 to 120 Vpp, the clot mass reduction will increase. The *in vitro* test results using MMBs with various ultrasound input parameters had a similar tendency with the previously reported sonothrombolysis results obtained by using microbubbles [29]. The input voltages range from 26 Vpp to 120 Vpp were selected according to our previous study [29]: the higher input voltages, the higher peak negative pressure (PNP) and mechanical index (MI) can be achieved. However, due to the ultrasound transducer material limitation (45% of the AC depoling voltage for PZT-5A ceramics), 120 Vpp was applied as an input voltage upper limit to keep the transducer working in a safe voltage range. The duty cycle ranges from 1.6% to 10% were used in this study according to our previous study [29]. The 10% (5 ms burst duration and 305 cycle-burst) was applied as a duty cycle upper limit to keep the transducer working in a safe range.

Next, we investigated the influence of magnetic field on the MMBs thrombolysis using the same ultrasound input parameter (120 V_{pp} input voltage, 6.4% duty cycle, 620 kHz). As shown in Fig. 9 (A), the higher magnetic field flux density, the higher clot mass reduction can be achieved. The possible reason can be explained as higher magnetic field flux density will induce the higher magnetic force applied on the magnetic microbubble, which will increase the vortex like microstreaming generated by the oscillating magnetic nanoparticles. To further investigate the influence of rotational magnetic field frequency on the lytic rate, we perform the *in vitro* test with different magnetic frequency from static, 1 Hz to 25 Hz. As shown in Fig. 9 (B), the lytic rate was increased when higher frequency rotational magnetic field applied to the magnetic microbubble. Which can be explained as higher frequency will increase the oscillation magnitude of magnetic microbubbles, and as a result, the magnetic microbubbles were more likely to be activated by the ultrasound and therefore induce more cavitation effect and microstreaming at the clot region.

3.5. Temperature changes and effects

To better understand the temperature changes and effects during the thrombolysis treatment, we measured the temperature changes of the clot region using a thermocouple probe. As shown in Fig. 10, the control group was only injected with saline without any ultrasound and magnetic field exposure. The MMB + RMF group is treated with magnetic microbubbles in a rotational magnetic field (B = 50 mT, f = 20 Hz). The temperature changes in MMB + RMF treatment group is not significant compared to the control group. This indicates that the rotational magnetic field in the low frequency range ($f < 25$ Hz) does not induce heating above the physiological temperature range. The MMB + US group and MMB + US + RMF group both have a slight temperature increase during the 30 min treatment. This is likely due to ultrasound exposure and the associated cavitation effects during the treatment. However, no significant change in temperature was observed in either MMB + US group or MMB + US + RMF group. This further indicates that the thrombolysis rate increase in the

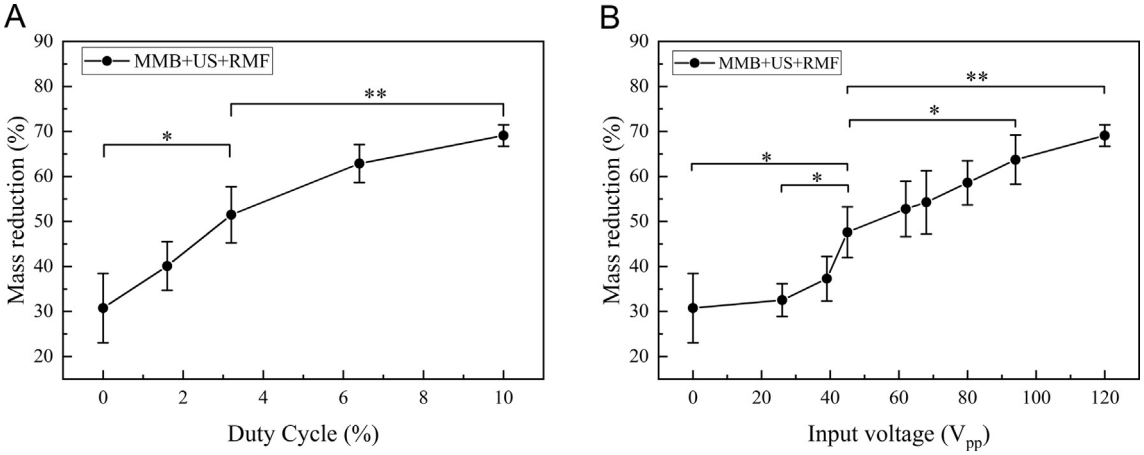

Fig. 8. *In vitro* test results using MMB + US + RMF treatment method with different ultrasound input (A) duty cycle, (B) input voltage (Treatment time:30 min, ultrasound parameters: f = 620 kHz, magnetic field: B = 50 mT, f = 20 Hz) (*$P < 0.05$, **$P < 0.01$).

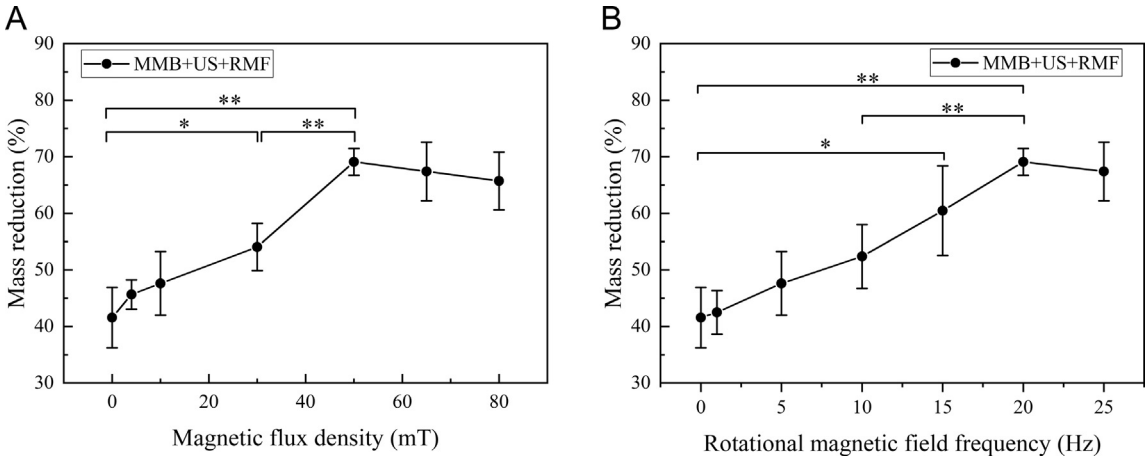

Fig. 9. *In vitro* test results using MMB + US + RMF treatment method with different magnetic field (A) flux density, (B) frequency (Treatment time: 30 min, ultrasound parameters: 120 V_{pp} input voltage, 10% duty cycle, f = 620 kHz) (*P < 0.05, **P < 0.01).

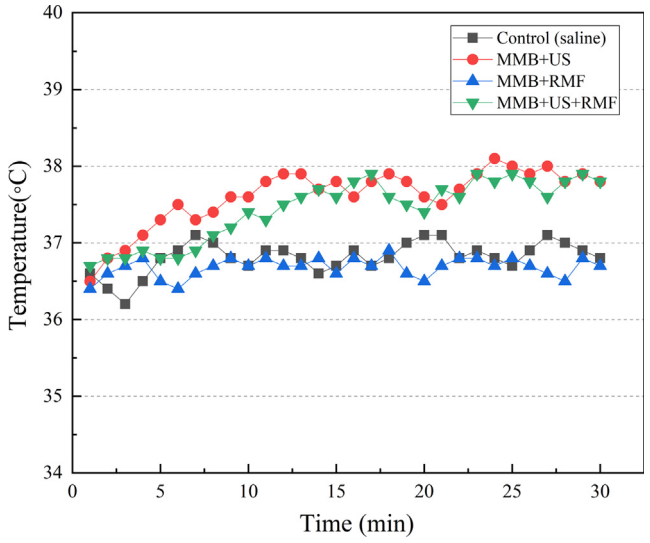

Fig. 10. Measured temperature changes of the clot region with different treatment methods. (Treatment time: 30 min, ultrasound parameters: 120 V_{pp} input voltage, 10% duty cycle, f = 620 kHz, magnetic field: B = 50 mT, f = 20 Hz).

MMB + US + RMF group is not mainly attributed by the temperature changes and effects.

3.6. The hypothesis of sonothrombolysis with MMBs under RMF

The hypothesis of magnetic microbubbles (MMBs) mediated intravascular sonothrombolysis by using a catheter-tipped forward-looking ultrasound transducer under a rotational magnetic field (RMF) is shown schematically in Fig. 11(A) and (B). First, the magnetic field can confine and trap the magnetic microbubbles around the clot region against blood flow and therefore increase the total concentration of magnetic microbubbles that retained at the clot surface for further ultrasound excitation. Second, when applied with the external rotational magnetic field, the magnetic microbubble will vibrate and oscillate at certain amplitude on the surface of the clot, resulting in a pair of counter-rotating vortices around the magnetic microbubbles, generating high shear flows, microjets, and microstreaming. Third, the fibrin network in the clot can be disrupted by the mechanical force generated from magnetic microbubble vibration and microstreaming under rotational magnetic field. Finally, the clot with disrupted fibrin network structure allows more magnetic microbubbles to diffuse beneath the clot surface and then magnetic microbubbles can be excited by ultrasound for cavitation to increase the clot lysis rate.

We hypothesize that sonothrombolysis with magnetic microbubbles using a catheter-tipped forward-looking ultrasound transducer under a rotational magnetic field is more advantageous for effective thrombolysis by enhancing the disruption of fibrin network of the clot and cavitation-induced microstreaming than the conventional high frequency, catheter-based thrombolysis techniques. The current techniques for treating thrombosis disease have many disadvantages such as low thrombolytic efficiency, hemorrhage, high failure rate, vein injury and the risk of distal embolism due to the large size of clot debris. Recently, the catheter-based side-looking intravascular ultrasound thrombolysis has demonstrated the improved lytic rate using high-frequency, low-power ultrasound waves that enhance the drug diffusion [43,44]. However, this method cannot be effective for thrombolysis without a thrombolytic agent. Moreover, the side looking method still needs a relatively long treatment time (> 10 h on average) with the use of high dose of the thrombolytic agent. In our approach, we initially realized a high thrombolysis rate (> 60% mass reduction) in a short time (30 min) in-vitro treatment without using any thrombolytic agent such as rt-PA. We anticipated that this approach could be a useful indicator of ultrasound-enhanced fibrinolysis by using rotational magnetic field in combination with magnetic microbubbles in a lower dose of rt-PA thrombolytic agent to achieve rapid thrombolysis treatment in the clinical application.

However, in the development of this sonothrombolysis technique, an advanced magnetic field generating system will be developed with higher magnetic flux density and frequency; the evaluation of the safety of the blood vessel wall and its surrounding tissue, clot debris size, and testing with rt-PA, etc. should also be carefully studied. Besides, different concentrations and size of MMBs need to be considered in future work.

3.7. The safety concerns of magnetic microbubbles

Regarding safety, the magnetic microbubbles (MMBs) are similar to those microbubbles (MBs) contrast agents that were used in the clinical applications and whose toxicity profile are well understood. However, the possible adverse effects of the presence of inorganic particles that were embedded in the MMBs as iron oxide magnetic nanoparticles must also be taken into consideration. Therefore, the potential risk of iron oxide nanoparticles in the human body is the most critical issue for investigation. From the toxicological point of view, the toxicity of magnetic nanoparticles may depend on many factors such as the dose, size, structure, chemical composition, surface and biodegradability [30].

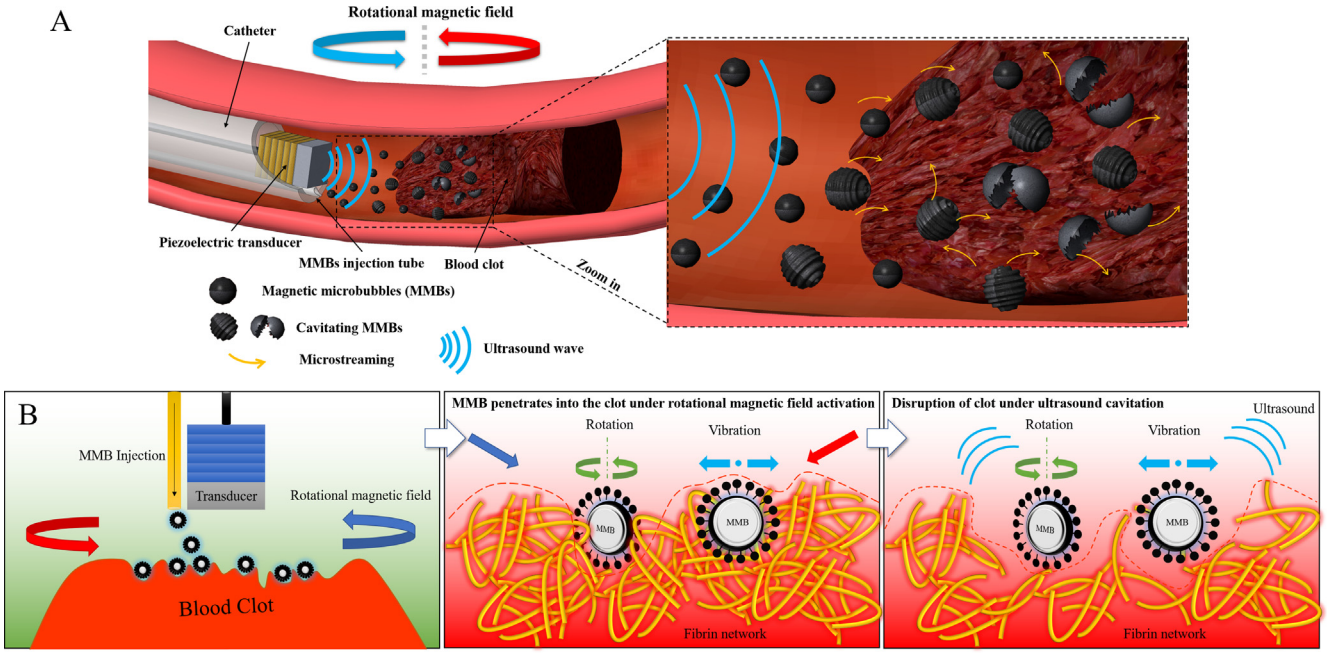

Fig. 11. Schematic view of sonothrombolysis with magnetic microbubbles under a rotational magnetic field. (A) MMBs are injected through the catheter and trapped near the clot region under the rotational magnetic field. (B) The hypothesis of sonothrombolysis with magnetic microbubbles under a rotational magnetic field. The MMBs can penetrate the clot surface and bind to the fibrin network of the clot under ultrasound exposure. When the rotational magnetic field is activated at this point, the MMBs start to rotate and vibrate, and the resulting shear force will cause the mechanical injury to the fibrin network. Then the MMBs can be activated by the ultrasound exposure and induce the cavitation effects, leading to the disruption of the clot.

First, as we know, size is the most crucial factor in the toxicity assessments of nanoparticles, and mostly the toxicity and size of nanoparticles are inversely related [31]; that is, the smaller the size of nanoparticles, the higher the toxicity. For example, iron oxide particles are well known to be non-toxic and are finally broken down to form blood hemoglobin inside the body. However, when it comes to the nanoscale size, the previous study demonstrated that the 30 nm sized iron oxide nanoparticles showed relatively higher toxicity compared to that of 500 nm sized particles [31].

Second, the influence of the surface coating is critical to the toxicity of nanoparticles. For example, the previous study showed that the uncoated iron oxide nanoparticles caused a significant decrease (by ~64%) in the human fibroblasts cell adhesion compared to that of control cells, but the PEG-coated nanoparticles did not cause much change [32]. Studies performed on the toxicity of magnetite-loaded polymeric particles have demonstrated that polymer coated nanoparticles had lower cytotoxicity than the uncoated magnetite nanoparticles. Moreover, many works have demonstrated that the biodegradable polymers were ideal nanoparticle surface coating materials since their minimum toxicity and the immunological response had been achieved [33,34]. Currently, in order to obtain microbubbles with high magnetic and acoustic sensitivities, iron oxide nanoparticles have been embedded into the shell of polymer and lipid-shelled microbubbles, encapsulated in the acoustically active lipospheres or the surface of the shell structures [35]. However, the embedded rigid nanoparticles will increase the stiffness of the microbubble's shell and reduce their sensitivity to ultrasound [36], while a surface coating of the microbubbles with some immunogenic material may lead to the shell destabilization [37]. As a result, the stiffening effects and surface destabilization of the magnetic microbubbles will increase the risks of pulmonary entrapment, which may cause further vascular occlusion and thromboembolism [38]. Recently, researchers have found that by attaching heparin-functionalized iron oxide nanoparticles to the surface of lipid-shelled microbubbles, both the compressibility and surface stealth of microbubbles could be preserved [21].

Third, the dose of the magnetic microbubble also plays a vital role in the safety of clinical application. A recent study has demonstrated that iron oxide nanoparticles with a concentration below 100 μg/ml could be safe and non-cytotoxic [39]. Another *in vitro* cytotoxicity study showed that the iron oxide nanoparticles are nontoxic at lower concentrations from 0.1 to 10 μg/ml while cytotoxicity could be found at 100 μg/ml [40]. The number of *in vivo* studies in the human body is very limited. However, the previous study found that a dextran-coated iron oxide nanoparticle only induced some mild side effects like urticaria and could be degraded and cleared from systemic circulation by the iron metabolic pathways [41,42].

In summary, the magnetic microbubbles may be considered as biocompatible. Nevertheless, their safety may vary with particle size, physicochemical composition, surface coating, dose range. To evaluate the safety of magnetic microbubbles, further optimization of the magnetic microbubble formulations and thrombolysis experimental conditions are necessary for the future.

4. Conclusions

In this study, we demonstrated that the additional use of magnetic microbubbles significantly enhances *in vitro* lysis of blood clot. First, we compared the influence of blood flow conditions on the different thrombolysis treatment methods (MB + US, MMB + US, MMB + RMF, MMB + US + RMF). Second, we investigated the influence of different vessel occlusion conditions (partial occlusion, fully occluded) and different clot ages (fresh, retracted) on the thrombolysis efficiency. Finally, to better understand the mechanism of rotational magnetic field assisted sonothrombolysis, we explored the influence of various ultrasound parameters (input voltage, duty cycle) and magnetic field parameters (amplitude, frequency) on the thrombolysis rate. This finding is especially attractive concerning future novel technology which may utilize the magnetic microbubbles to treat and optimize the thrombolysis of *in vivo* intravascular occlusions.

Acknowledgment

Funding: This work was supported in part by the National Institutes of Health [grant numbers R01HL141967]. The author would like to thank Leela Goel for proofreading of the manuscript.

Declaration of Competing Interest

Xiaoning Jiang has a financial interest in SonoVascular, Inc.

References

[1] E.J. Benjamin, S.S. Virani, C.W. Callaway, A.M. Chamberlain, A.R. Chang, S. Cheng, S.E. Chiuve, M. Cushman, F.N. Delling, R. Deo, S.D. De Ferranti, J.F. Ferguson, M. Fornage, C. Gillespie, C.R. Isasi, M.C. Jiménez, L.C. Jordan, S.E. Judd, D. Lackland, J.H. Lichtman, L. Lisabeth, S. Liu, C.T. Longenecker, P.L. Lutsey, J.S. MacKey, D.B. Matchar, K. Matsushita, M.E. Mussolino, K. Nasir, M. O'Flaherty, L.P. Palaniappan, A. Pandey, D.K. Pandey, M.J. Reeves, M.D. Ritchey, C.J. Rodriguez, G.A. Roth, W.D. Rosamond, U.K.A. Sampson, G.M. Satou, S.H. Shah, N.L. Spartano, D.L. Tirschwell, C.W. Tsao, J.H. Voeks, J.Z. Willey, J.T. Wilkins, J.H.Y. Wu, H.M. Alger, S.S. Wong, P. Muntner, Heart disease and stroke statistics - update: A report from the American Heart Association, Circulation. 137 (2018) (2018) E67–E492, https://doi.org/10.1161/CIR.0000000000000558.

[2] T. Truelsen, S. Begg, C. Mathers, The global burden of cerebrovascular disease, Glob. Burd. Dis. (2005) 1–67, https://doi.org/10.2135/cropsci2003.0425.

[3] J.H. Rha, J.L. Saver, The impact of recanalization on ischemic stroke outcome: A meta-analysis, Stroke 38 (2007) 967–973, https://doi.org/10.1161/01.STR.0000258112.14918.24.

[4] W. Hacke, M. Kaste, E. Bluhmki, M. Brozman, A. Dávalos, D. Guidetti, V. Larrue, K.R. Lees, Z. Medeghri, T. Machnig, D. Schneider, R. von Kummer, N. Wahlgren, D. Toni, Thrombolysis with Alteplase 3 to 4.5 Hours after Acute Ischemic Stroke, N. Engl. J. Med. 359 (2008) 1317–1329, https://doi.org/10.1056/NEJMoa0804656.

[5] T.N.I. of N.D. and S. rt-P.S.S. Group, Tissue Plasminogen Activator for Acute Ischemic Stroke, N. Engl. J. Med. 333 (1995) 1581–1588. http://doi.org/10.1056/NEJM199512143332401.

[6] J. Edlow, Clinical policy: Use of intravenous tPA for the management of acute ischemic stroke in the emergency department, Ann. Emerg. Med. 61 (2013) 225–243, https://doi.org/10.1016/j.annemergmed.2012.11.005.

[7] B.C.V. Campbell, P.J. Mitchell, T.J. Kleinig, H.M. Dewey, L. Churilov, N. Yassi, B. Yan, R.J. Dowling, M.W. Parsons, T.J. Oxley, T.Y. Wu, M. Brooks, M.A. Simpson, F. Miteff, C.R. Levi, M. Krause, T.J. Harrington, K.C. Faulder, B.S. Steinfort, M. Priglinger, T. Ang, R. Scroop, P.A. Barber, B. McGuinness, T. Wijeratne, T.G. Phan, W. Chong, R.V. Chandra, C.F. Bladin, M. Badve, H. Rice, L. de Villiers, H. Ma, P.M. Desmond, G.A. Donnan, S.M. Davis, Endovascular therapy for ischemic stroke with perfusion-imaging selection, N. Engl. J. Med. 372 (2015) 1009–1018, https://doi.org/10.1056/NEJMoa1414792.

[8] S. Ricci, L. Dinia, M. Del Sette, P. Anzola, T. Mazzoli, S. Cenciarelli, C. Gandolfo, Sonothrombolysis for acute ischaemic stroke, Cochrane Database Syst. Rev. (2012), https://doi.org/10.1002/14651858.CD008348.pub3.

[9] O.A. Berkhemer, P.S.S. Fransen, D. Beumer, L.A. van den Berg, H.F. Lingsma, A.J. Yoo, W.J. Schonewille, J.A. Vos, P.J. Nederkoorn, M.J.H. Wermer, M.A.A. van Walderveen, J. Staals, J. Hofmeijer, J.A. van Oostayen, G.J. Lycklama à Nijeholt, J. Boiten, P.A. Brouwer, B.J. Emmer, S.F. Debruijn, L.C. van Dijk, L.J. Kappelle, R.H. Lo, E.J. van Dijk, J. de Vries, P.L.M. de Kort, W.J.J. van Rooij, J.S.P. van den Berg, B.A.A.M. van Hasselt, L.A.M. Aerden, R.J. Dallinga, M.C. Visser, J.C.J. Bot, P.C. Vroomen, O. Eshghi, T.H.C.M.L. Schreuder, R.J.J. Heijboer, K. Keizer, A.V. Tielbeek, H.M. den Hertog, D.G. Gerrits, R.M. van Denberg-Vos, G.B. Karas, E.W. Steyerberg, H.Z. Flach, H.A. Marquering, M.E.S. Sprengers, S.F.M. Jenniskens, L.F.M. Beenen, R. van den Berg, P.J. Koudstaal, W.H. van Zwam, Y.B.W.E.M. Roos, A. van der Lugt, R.J. van Oostenbrugge, C.B.L.M. Majoie, D.W.J. Dippel, A randomized trial of intraarterial treatment for acute ischemic stroke, N. Engl. J. Med. 372 (2014) 11–20, https://doi.org/10.1056/NEJMoa1411587.

[10] L. Auboire, C.A. Sennoga, J.M. Hyvelin, F. Ossant, J.M. Escoffre, F. Tranquart, A. Bouakaz, Microbubbles combined with ultrasound therapy in ischemic stroke: A systematic review of in-vivo preclinical studies, PLoS One 13 (2018) e0191788, https://doi.org/10.1371/journal.pone.0191788.

[11] T.R. Porter, R.F. LeVeen, R. Fox, A. Kricsfeld, F. Xie, Thrombolytic enhancement with perfluorocarbon-exposed sonicated dextrose albumin microbubbles, Am. Heart J. 132 (1996) 964–968, https://doi.org/10.1016/S0002-8703(96)90006-X.

[12] S. Datta, C.C. Coussios, A.Y. Ammi, T.D. Mast, G.M. de Courten-Myers, C.K. Holland, Ultrasound-enhanced thrombolysis using Definity® as a cavitation nucleation agent, Ultrasound Med. Biol. 34 (2008) 1421–1433, https://doi.org/10.1016/j.ultrasmedbio.2008.01.016.

[13] A. Angelika, D.M. Alberto, S. Mark, F. Marc, G. Martin, P. Sibylle, S. Michel, H. Michael, A. Eric, M. Stephen, Molecular imaging of human thrombus with novel abciximab immunobubbles and ultrasound, Stroke 38 (2007) 1508–1514, https://doi.org/10.1161/STROKEAHA.106.471391.

[14] F. Xie, J. Lof, T. Matsunaga, R. Zutshi, T.R. Porter, Diagnostic ultrasound combined with glycoprotein IIb/IIIa-targeted microbubbles improves microvascular recovery after acute coronary thrombotic occlusions, Circulation 119 (2009) 1378–1385, https://doi.org/10.1161/CIRCULATIONAHA.108.825067.

[15] M.J. Martin, E.M.L. Chung, A.H. Goodall, A. Della Martina, K.V. Ramnarine, L. Fan, S.V. Hainsworth, A.R. Naylor, D.H. Evans, Enhanced detection of thromboemboli with the use of targeted microbubbles, Stroke 38 (2007) 2726–2732, https://doi.org/10.1161/STROKEAHA.107.489435.

[16] P.A. Schumann, J.P. Christiansen, R.M. Quigley, T.P. McCreery, R.H. Sweitzer, E.C. Unger, J.R. Lindner, T.O. Matsunaga, Targeted-microbubble binding selectively to GPIIb IIIa receptors of platelet thrombi, Invest. Radiol. 37 (2002) 587–593, https://doi.org/10.1097/00004424-200211000-00001.

[17] X. Wang, C.E. Hagemeyer, J.D. Hohmann, E. Leitner, P.C. Armstrong, F. Jia, M. Olschewski, A. Needles, K. Peter, I. Ahrens, Novel single-chain antibody-targeted microbubbles for molecular ultrasound imaging of thrombosis: Validation of a unique noninvasive method for rapid and sensitive detection of thrombi and monitoring of success or failure of thrombolysis in mice, Circulation 125 (2012) 3117–3126, https://doi.org/10.1161/CIRCULATIONAHA.111.030312.

[18] P. Dayton, A. Klibanov, G. Brandenburger, K. Ferrara, Acoustic radiation force in vivo: A mechanism to assist targeting of microbubbles, Ultrasound Med. Biol. 25 (1999) 1195–1201, https://doi.org/10.1016/S0301-5629(99)00062-9.

[19] S. Zhao, M. Borden, S.H. Bloch, D. Kruse, K.W. Ferrara, P.A. Dayton, Radiation-force assisted targeting facilitates ultrasonic molecular imaging, Mol. Imaging 3 (2004) 135–148, https://doi.org/10.1162/1535350042380317.

[20] J.J. Rychak, A.L. Klibanov, K.F. Ley, J.A. Hossack, Enhanced targeting of ultrasound contrast agents using acoustic radiation force, Ultrasound Med. Biol. 33 (2007) 1132–1139, https://doi.org/10.1016/j.ultrasmedbio.2007.01.005.

[21] B. Chertok, R. Langer, Circulating magnetic microbubbles for localized real-time control of drug delivery by ultrasonography-guided magnetic targeting and ultrasound, Theranostics 8 (2018) 341–357, https://doi.org/10.7150/thno.20781.

[22] M. De Saint Victor, D. Carugo, L.C. Barnsley, J. Owen, C.C. Coussios, E. Stride, Magnetic targeting to enhance microbubble delivery in an occluded microarterial bifurcation, Phys. Med. Biol. 62 (2017) 7451–7470, https://doi.org/10.1088/1361-6560/aa858f.

[23] A.S. Drozdov, V.V. Vinogradov, I.P. Dudanov, V.V. Vinogradov, Leach-proof magnetic thrombolytic nanoparticles and coatings of enhanced activity, Sci. Rep. 6 (2016) 28119, https://doi.org/10.1038/srep28119.

[24] Y. Gao, C.U. Chan, Q. Gu, X. Lin, W. Zhang, D.C.L. Yeo, A.M. Alsema, M. Arora, M.S.K. Chong, P. Shi, C.D. Ohl, C. Xu, Controlled nanoparticle release from stable magnetic microbubble oscillations, NPG Asia Mater. 8 (2016) e260–e310, https://doi.org/10.1038/am.2016.37.

[25] H. Mannell, J. Pircher, F. Fochler, Y. Stampnik, T. Räthel, B. Gleich, C. Plank, O. Mykhaylyk, C. Dahmani, M. Wörnle, A. Ribeiro, U. Pohl, F. Krötz, Site directed vascular gene delivery in vivo by ultrasonic destruction of magnetic nanoparticle coated microbubbles, Nanomedicine Nanotechnology, Biol. Med. 8 (2012) 1309–1318, https://doi.org/10.1016/j.nano.2012.03.007.

[26] M.D. Torno, M.D. Kaminski, Y. Xie, R.E. Meyers, C.J. Mertz, X. Liu, W.D. O'Brien, A.J. Rosengart, Improvement of in vitro thrombolysis employing magnetically-guided microspheres, Thromb. Res. 121 (2008) 799–811, https://doi.org/10.1016/j.thromres.2007.08.017.

[27] F. Bi, J. Zhang, Y. Su, Y.C. Tang, J.N. Liu, Chemical conjugation of urokinase to magnetic nanoparticles for targeted thrombolysis, Biomaterials 30 (2009) 5125–5130, https://doi.org/10.1016/j.biomaterials.2009.06.006.

[28] J. Owen, P. Rademeyer, D. Chung, Q. Cheng, D. Holroyd, C. Coussios, P. Friend, Q.A. Pankhurst, E. Stride, Magnetic targeting of microbubbles against physiologically relevant flow conditions, Interface Focus. 5 (2015) 1–12, https://doi.org/10.1098/rsfs.2015.0001.

[29] J. Kim, B.D. Lindsey, W.Y. Chang, X. Dai, J.M. Stavas, P.A. Dayton, X. Jiang, Intravascular forward-looking ultrasound transducers for microbubble-mediated sonothrombolysis, Sci. Rep. 7 (2017) 1–10, https://doi.org/10.1038/s41598-017-03492-4.

[30] M. Arruebo, R. Fernández-Pacheco, M.R. Ibarra, J. Santamaría, Magnetic nanoparticles for drug delivery, Nano Today 2 (2007) 22–32, https://doi.org/10.1016/S1748-0132(07)70084-1.

[31] H.L. Karlsson, J. Gustafsson, P. Cronholm, L. Möller, Size-dependent toxicity of metal oxide particles—A comparison between nano- and micrometer size, Toxicol. Lett. 188 (2009) 112–118, https://doi.org/10.1016/J.TOXLET.2009.03.014.

[32] A.K. Gupta, A.S.G. Curtis, Surface modified superparamagnetic nanoparticles for drug delivery: Interaction studies with human fibroblasts in culture, J. Mater. Sci. Mater. Med. 15 (2004) 493–496, https://doi.org/10.1023/B:JMSM.0000021126.32934.20.

[33] H. Otsuka, Y. Nagasaki, K. Kataoka, PEGylated nanoparticles for biological and pharmaceutical applications, Adv. Drug Deliv. Rev. 55 (2003) 403–419, https://doi.org/10.1016/S0169-409X(02)00226-0.

[34] A. Chilkoti, M.R. Dreher, D.E. Meyer, Design of thermally responsive, recombinant polypeptide carriers for targeted drug delivery, Adv. Drug Deliv. Rev. 54 (2002) 1093–1111, https://doi.org/10.1016/S0169-409X(02)00060-1.

[35] F. Yang, Y. Li, Z. Chen, Y. Zhang, J. Wu, N. Gu, Superparamagnetic iron oxide nanoparticle-embedded encapsulated microbubbles as dual contrast agents of magnetic resonance and ultrasound imaging, Biomaterials 30 (2009) 3882–3890, https://doi.org/10.1016/j.biomaterials.2009.03.051.

[36] D. Vlaskou, O. Mykhaylyk, F. Krötz, N. Hellwig, R. Renner, U. Schillinger, B. Gleich, A. Heidsieck, G. Schmitz, K. Hensel, C. Plank, Magnetic and acoustically active lipospheres for magnetically targeted nucleic acid delivery, Adv. Funct. Mater. 20 (2010) 3881–3894, https://doi.org/10.1002/adfm.200902388.

[37] C.C. Chen, M.A. Borden, The role of poly(ethylene glycol) brush architecture in complement activation on targeted microbubble surfaces, Biomaterials 32 (2011) 6579–6587, https://doi.org/10.3233/MAS-2012-0234.

[38] Å. Barrefelt, M. Saghafian, R. Kuiper, F. Ye, G. Egri, M. Klickermann, T.B. Brismar, P. Aspelin, M. Muhammed, L. Dähne, M. Hassan, Biodistribution, kinetics, and biological fate of SPION microbubbles in the rat, Int. J. Nanomed. 8 (2013)

3241–3254, https://doi.org/10.2147/IJN.S49948.
[39] H.L. Karlsson, P. Cronholm, J. Gustafsson, L. Möller, Copper oxide nanoparticles are highly toxic: a comparison between metal oxide nanoparticles and carbon nanotubes, Chem. Res. Toxicol. 21 (2008) 1726–1732, https://doi.org/10.1021/tx800064j.
[40] B. Ankamwar, T.C. Lai, J.H. Huang, R.S. Liu, M. Hsiao, C.H. Chen, Y.K. Hwu, Biocompatibility of Fe_3O_4 nanoparticles evaluated by in vitro cytotoxicity assays using normal, glia and breast cancer cells, Nanotechnology 21 (2010) 75102, https://doi.org/10.1088/0957-4484/21/7/075102.
[41] Y. Anzai, C.W. Piccoli, E.K. Outwater, W. Stanford, D.A. Bluemke, P. Nurenberg, S. Saini, K.R. Maravilla, D.E. Feldman, U.P. Schmiedl, J.A. Brunberg, I.R. Francis, S.E. Harms, P.M. Som, C.M. Tempany, Group, Evaluation of neck and body metastases to nodes with ferumoxtran 10-enhanced MR imaging: phase III safety and efficacy study, Radiology 228 (2003) 777–788, https://doi.org/10.1148/radiol.2283020872.
[42] R. Weissleder, D.D. Stark, B.L. Engelstad, B.R. Bacon, C.C. Compton, D.L. White, P. Jacobs, J. Lewis, Superparamagnetic iron oxide: pharmacokinetics and toxicity, AJR. Am. J. Roentgenol. 152 (1989) 167–173, https://doi.org/10.2214/ajr.152.1.167.
[43] C.A. Owens, Ultrasound-enhanced thrombolysis: EKOS EndoWave infusion catheter system, Semin. Intervent. Radiol. 25 (2008) 37–41, https://doi.org/10.1055/s-2008-1052304.
[44] N. Kucher, P. Boekstegers, O.J. Müller, C. Kupatt, J. Beyer-Westendorf, T. Heitzer, U. Tebbe, J. Horstkotte, R. Müller, E. Blessing, M. Greif, P. Lange, R.-T. Hoffmann, S. Werth, A. Barmeyer, D. Härtel, H. Grünwald, K. Empen, I. Baumgartner, Randomized, controlled trial of ultrasound-assisted catheter-directed thrombolysis for acute intermediate-risk pulmonary embolism, Circulation 129 (2014) 479–486, https://doi.org/10.1161/CIRCULATIONAHA.113.005544.